# Load Flow Models for the Static Var Compensator Distribution D-SVC

LARBI BOUMEDIENE, MOUNIR KHIAT, MUSTAPHA RAHLI
Electrical Engineering, Electrical Engineering, Electrical Engineering
University Center Moulay Tahar of Saida, High National School of Technical Teaching Oran, University
of Science and Technology of Oran -Mohamed Boudiaf-.
BP 138 En-Nasr, Saida, ALGFERIA, BP 1523 M'nouaer, Oran –ALGFERIA,
BP 1505 El Mnaouer -Oran - ALGFERIA
lboumediene2005@yahoo.fr

*Abstract:* - During the last decade power system have been equipped with complex components such as Distribution Static Var Compensators (D-SVCs). These components have introduced new possibilities to control power systems, D-SVCs can almost continuously change the amount of reactive power from capacitor banks. The behavior of these new components is different from 'old' technologies since they contain power electronics and detailed representations of them are non-linear. Due to their complexity they are difficult also to simulate. When studying power systems including such components, the analyzer must decide whether it is necessary to include a detailed model of them or not, i.e. to represent each event that takes place, or ignore them. In this paper, the load flow models for the static Var compensator distribution (D-SVC) are presented. These models are incorporated into existing load flow harmonic (LFH). The models of the D-SVC are based instead on the variable shunt susceptance concept. The D-SVC state variables are combined with the bus voltage magnitudes and angles of the network. Two examples are examined in the principal content of this paper; both of them contain nonlinear loads. Conclusion is made concerning the application of harmonic power flow studies.

## 1 Introduction

In electric power systems, bus voltages are significantly affected by load variations and by network topology changes. Voltages can drop considerably and even collapse when the network is operating under heavy loading. This may trigger the operation of under-voltage relays and other voltage sensitive controls, leading to extensive disconnection of loads and thus adversely affecting consumers and company revenue. On the other hand, when the load level in the system is low, over-voltages can arise due to Ferranti effect. Capacitive over-compensation and over-excitation of synchronous machines can also occur. Over-voltages cause equipment failures due to insulation breakdown and produce magnetic saturation in transformers, resulting in harmonic generation. Hence, voltage magnitude throughout the network cannot deviate significantly from its nominal value if an efficient and reliable operation of the power system is to be achieved. Voltage regulation is achieved by controlling the production, absorption and flow of reactive power throughout the network.

This device is essentially a variable reactor that can adjust its reactive power consumption. The adjustment is realised through the firing angles of thyristors that normally operate in partial conducting states, and thereby produce harmonics (Miller 1982).

The generated harmonics depend critically on the control characteristics of a static distribution VAR compensator (D-SVC) with a thyristor-controlled reactor (TCR). However this makes the firing angles dependent on the network load flow conditions and harmonic voltage distributions (Xu et al 1991). Poor selection of firing angles can lead to increase in the amount of effective harmonic production of the TCR. From the operation point of view of the system, we need to model the harmonics accurately (Uzunoglu et al 1999).

Static VAR compensators (D-SVCs) are applied on systems to improve voltage control and system stability during both normal and contingency system conditions [6].

The technical literature is populated with clever and elegant solutions for accommodating models of controllable plant in Newton–Raphson power flow algorithms; load tap-changing and phase-shifting transformers are typical examples of such work. The modelling approach used to represent controllable equipment can be broadly classified into two main

categories, namely, sequential and simultaneous solution methods [1].

The objective of this paper is to solve the network at fundamental and harmonic frequencies in the presence of nonlinear elements and unbalances with a harmonic load flow technique and to present a D-SVC model for flexible and robustness integration in harmonic power flow under balanced conditions. This integration is based in a fixed point iteration-Newton procedure for the conventional load flow (CLF).The D-SVC models have been tested in a wide range of power networks of varying sizes.

## 2  D-SVC Load Flow Models

In its simplest form, the D-SVC consists of a TCR in parallel with a bank of capacitors pictured in Fig 1. From an operational point of view, the D-SVC behaves like a shunt connected variable reactance, which either generates or absorbs reactive power in order to regulate the voltage magnitude at the point of connection to the AC network. It is used extensively to provide fast reactive power and voltage regulation support. The firing angle control of the thyristor enables the D-SVC to have almost instantaneous speed of response.

The lowest harmonic orders reaching the primary winding of the transformer are $h = 11$, 13, which are normally removed by using tuned filters, satisfying constraint conditions.
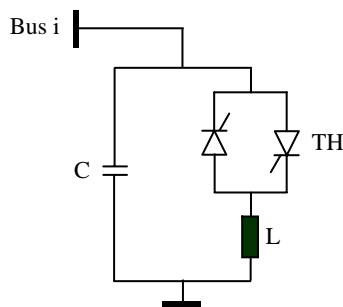


**Fig.1** D-SVC circuit.

The D-SVC is taken to be a variable-shunt susceptance, which is adjusted in order to achieve a specified voltage magnitude while satisfying constraint conditions. We will use three models of D-SVC.

1. DSVC injection model.
2. D-SVC total susceptance model.
3. D-SVC firing angle model.

### 2.1 The Injection Model
The model of injection describes the FACTS as device which injects a quantity of reactive power $Q$ to a bus, in this case the FACTS is represented like

$P/Q$ element with $P = 0$. The model can be applied in the calculation of the load flow and in the calculation of the optimal power flow.

In this model, it is independent of the internal design of the FACTS.

### 2.2  Shunt Variable Susceptance Model
In practice, the D-SVC can be seen as an adjustable reactance with either firing-angle limits or reactance limits. The equivalent circuit is used to derive the D-SVC nonlinear power equations and the linearised equations required by Newton's method.

The changing susceptance represents the total D-SVC susceptance necessary to maintain the bus voltage magnitude at the specified value.
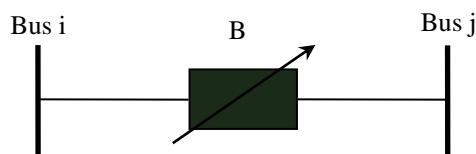


Fig.2 Total susceptance model

This model interprets the FACTS as a shunt (for shunt compensation) or series element (for series compensation), the power flow through the FACTS depends on $B$, $P_{ij}$ and $Q_{ij} = f(B)$ .Fig 2 shows a 1-port and 2-port black box. In network analysis every n port is represented by the impedance matrix which can be stated from the T or $\Pi$ circuit model of the network of element. Inserting the variable $B$ in the 1- and 2-port models for shunt and series element leads to the 1-port matrix model for the shunt connected element.

$$[I_i] - \lfloor jB_{ij} \rfloor [U_i] = [0] \tag{1}$$
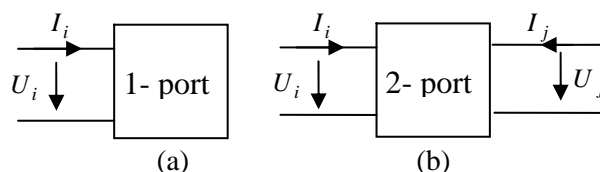


**Fig.3** 1-port (a) and 2-port (b) element

The 2-port model for the series element can be stated as:

$$\begin{bmatrix} I_i \\ I_j \end{bmatrix} - \begin{bmatrix} -jB_{ij} & jB_{ij} \\ jB_{ij} & -jB_{ij} \end{bmatrix} \begin{bmatrix} U_i \\ U_J \end{bmatrix} = \begin{bmatrix} 0 \\ 0 \end{bmatrix} \tag{2}$$

Since it is well know how to implement the 1-port and 2-port models in a power flow computation, this model is proper for a power flow computation with Newton-Raphson. Like the Injection Model, the Total Susceptance Model does not describe the internal design of the

FACTS. It does not contain the dependence of B from any internal value, for example firing angle.

## 2.3 Firing-angle Model

An alternative D-SVC model, which avoids the additional iterative process, consists in handling the firing angle $\alpha$ of the thyristor-controlled reactor (TCR) as a state variable in the power flow formulation.

The Firing Angle Model includes the dependence of the FACTS impedance or power values from the variable firing angles of semiconductor switches.

The firing angle is now considered as a state variable, so that $B_{ij}^{-1} = X_{ij} = f(\alpha, X_L, X_C)$ and $P_{ij}, Q_{ij} = f(\alpha, X_L, X_C)$. Such a function $f(\alpha, X_L, X_C)$ can be inserted in the injection model as well as the total susceptance model.

With the firing angle model, we consider the internal circuit as well as values which affect the power flow through the device, like capacitance, reactance and especially the firing angle.

## 3 Bus voltage magnitude control using D-Svc

The D-SVC connecting bus is a voltage-controlled bus where the voltage magnitude and active and reactive powers are specified and either the D-SVC firing angle, $\alpha_{D-SVC}$, or the D-SVC equivalent susceptance, $B_{D-SVC}$, are handled as state variables. This bus is defined to be *PVB* type. If $\alpha_{D-SVC}$ or $\beta_{D-SVC}$ are within limits, the specified voltage magnitude is attained and the controlled bus remains *PVB*. However, if $\alpha_{D-SVC}$ or $\beta_{D-SVC}$ go outside the limits then these variables are fixed at the violated limit and the bus becomes *PQ*. This is, of course, in the absence of any other controller capable of providing reactive power control at the bus.

At harmonic frequencies, the equivalent currents $I_{h-eq}$ representing the effects of nonlinear elements are set to zero. For the fundamental frequency load flow solutions, the *PV* and *PQ* components are modified into known *Y* matrices. With these simplifications, the approximate bus voltages without harmonic distortion $(h = 1)$ are obtained in one-iteration. Because the voltage harmonics are relatively small compared with the fundamental frequency components, using the bus voltages as initial conditions is quite reliable.

The technique consists of two basic parts. The first part is the construction of harmonic equivalent circuits for the nonlinear elements (a TCR is used as an example). The second part performs the network solutions at the fundamental and harmonic frequencies. These two parts are interfaced through the process of harmonic iteration.

## 4 Harmonic power flow algorithm

Network voltages and currents can be expressed by Fourier series for the harmonic power flow analysis, which was developed by Xia and Heydt [4]. Voltages and nonlinear element parameters form the bus variable vector $(\phi)$, are given as,[2].

$$[X] = \left[[V^{(1)}],[V^{(5)}],...........,[V^{(h)}],[\phi]\right]^T \quad (3)$$

In this equation, $L$ is the maximum harmonic order. The mismatch of real and reactive powers for the linear buses (while $k \in \{2,...,(m-1)\}$) is defined as,

$$\left.\begin{array}{l} \Delta P_k = (P_k)_{sp} + F_{p,k}^{(1)} \\ \Delta Q_k = (Q_k)_{sp} + F_{q,k}^{(1)} \end{array}\right\} \quad (4)$$

Where $m$ is the first nonlinear load number and the first bus is the slack bus.
$(P_k)sp$ and $(Q_k)sp$ are real and reactive powers at bus k respectively, and $F_{r,k}^{(1)}$ and $F_{i,k}^{(1)}$ are the line fundamental real and reactive powers. The mismatch of real and reactive powers can be calculated for nonlinear buses as,

$$\left.\begin{array}{l} \Delta P_k^{nonlinear} = (P_k)_{sp} + \sum_{h=1}^{L} F_{p,k}^{(h)} \\ \Delta Q_k^{nonlinear} = (Q_k)_{sp} + \sum_{h=1}^{L} F_{q,k}^{(1)} \end{array}\right\} \quad (5)$$

Where $k \in \{m, m+1,...,n\}$ and $n$ is total number of the buses in the system $F_{p,k}^{(h)}$ and $F_{q,k}^{(h)}$ can be calculated from (for $h = 1,5,7,...,L$).

$$\left.\begin{array}{l} F_{p,k}^{h} = V_k^{(h)} \sum_{j=1}^{n} Y_{jk}^{h}.V_j^{(h)}.\cos(\delta_k^{(h)} - \theta_{kj}^{(h)} - \delta_j^{(h)}) \\ F_{q,k}^{h} = V_k^{(h)} \sum_{j=1}^{n} Y_{jk}^{h}.V_j^{(h)}.\sin(\delta_k^{(h)} - \theta_{kj}^{(h)} - \delta_j^{(h)}) \end{array}\right\} \quad (6)$$

The harmonic phase voltage for $k^{th}$ bus is $V_k^{(h)} = V_k^{(h)} \angle \delta_k^{h}$ and element $(k,j)$ of the bus admittance matrix for the $h^{th}$ harmonic frequency is shown in phase notation as $Y_k^{(h)} = Y_{kj}^{(h)} \angle \theta_{kj}^{h}$. Here, the mismatch vector for the harmonic power flow is defined as [8].

$$[\Delta M] = \left[[\Delta W],[\Delta I^{(5)}],[\Delta I^{(7)}],..,[\Delta I^{(L)}][\Delta I^{(1)}]\right]^T \quad (7)$$

Where $\Delta W$ is the mismatch power vector and $\Delta I^{(h)}$ is the mismatch current vector for the $h^{th}$ harmonic. The mismatch power is given by,

$$[\Delta M] = [\Delta P_2, \Delta Q_2, ..., \Delta P_{m-1}, \Delta P_m^{nonlin},$$
$$\Delta Q_m^{nonlin}, ..., \Delta P_n^{nonlin}, \Delta Q_n^{nonlin}] \qquad (8)$$

The mismatch current vector for the fundamental component ($h=1$) and the harmonic components ($h = 5, 7, ..., L$), which are the elements of the mismatch vector is given respectively by:

$$[\Delta I^{(1)}] = \left[\left(I_{r,m}^{(1)} + g_{r,m}^{(1)}\right), \left(I_{i,m}^{(1)} + g_{i,m}^{(1)}\right),\right.$$
$$\left(I_{r,m+1}^{(1)} + g_{r,m+1}^{(1)}\right), \left(I_{i,m+1}^{(1)} + g_{i,m+1}^{(1)}\right) \qquad (9)$$
$$\left.\dots, \left(I_{r,n}^{(1)} + g_{r,n}^{(1)}\right), \left(I_{i,n}^{(1)} + g_{i,n}^{(1)}\right)\right]$$

$$[\Delta I^{(h)}] = \left[I_{r,1}^{(h)}, I_{i,1}^{(h)}, ..., I_{r,m-1}^{(h)}, I_{i,m-1}^{(h)},\right.$$
$$\left(I_{r,m}^{(h)} + g_{r,m}^{(h)}\right), \left(I_{i,m}^{(h)} + g_{i,m}^{(h)}\right)$$
$$\left(I_{r,m+1}^{(h)} + g_{r,m+1}^{(h)}\right), \left(I_{i,m+1}^{(h)} + g_{i,m+1}^{(h)}\right)... \qquad (10)$$
$$\left.\left(I_{r,n}^{(h)} + g_{r,n}^{(h)}\right), \left(I_{i,n}^{(h)} + g_{i,n}^{(h)}\right)\right]$$

In these equations, $I_{r,k}^{(h)}$ and $I_{i,k}^{(h)}$ are to be zero for the harmonic components at linear buses ($k = 1, 2, ..., m-1$).

## 4.1 Reformulation of the Newton Raphson method to allow for harmonics

Before proceeding to the principal objective of this paper the reformulation of the power flow problem to include harmonics, it is necessary to investigate the tension and current relation ships at nonlinear buses.

In the reformulation of the power flow problem below, it will be assumed that the load apparent volt-amperes at non linear load buses are know [3].

Having completed this analysis, it will be possible to proceed directly to the reformulation of the power flow study. The load phase currents are expressed in Fourier series with odd terms only.

$$i(t) = \sum_l (i_i^l \cos l\omega t + i_r^l \sin l\omega t) \qquad (11)$$

$$l = 1, 5, 7, 11, 13, .....$$

$$i_i^l = 2/\pi \int_\alpha^{\pi+\alpha} i_a(t) \cos l\omega t \, d\omega t \qquad (12)$$

$$i_i^l = 2/\pi \int_\alpha^{\pi+\alpha} i_a(t) \sin l\omega t \, d\omega t \qquad (13)$$

Then the integration in (12-13) is divided in to six periods in each of which $i_a(t)$ is known and presented in some detail in [3]. After calculation, we found the results of the currents.

$$I_{i,s}^l = \frac{2}{\pi} \sum_m \left[\sum_k \frac{Y_k^{(m)} u_k}{2} \left[\frac{\cos((k+l)\omega t + \Phi_k + \theta_k^{(m)})}{-k-l}\right]\right.$$
$$+ \left[\sum_k^{\neq l} \frac{Y_k^m u_k}{2} \left[\frac{\cos((k-l)\omega t + \Phi_k + \theta_k^{(m)})}{-k+l}\right.\right.$$
$$\left.+ \frac{Y_l^{(m)} u_l}{2} t \sin(\phi_l + \theta_l^{(m)})\right]$$

$$I_{r,s}^l = \frac{2}{\pi} \sum_m \left[\sum_k \frac{Y_k^{(m)} u_k}{2} \left[\frac{\sin((k+l)\omega t + \Phi_k + \theta_k^{(m)})}{-k-l}\right]\right.$$
$$+ \left[\sum_k^{\neq l} \frac{Y_k^m u_k}{2} \left[\frac{\sin((k-l)\omega t + \Phi_k + \theta_k^{(m)})}{k-l}\right.\right.$$
$$\left.+ \frac{Y_l^{(m)} u_l}{2} t \cos(\phi_l + \theta_l^{(m)})\right] \qquad (14)$$

The objective of this paragraph, but note that the partial derivatives of $I_{i,t}^{(l)}$ through $I_{r,s}^{(t)}$ will be required in Newton–Raphson method power flow solution.

The Newton–Raphson method can be applied to harmonic current flow. This is based on the balance of active and reactive powers, whether at fundamental frequency or at harmonics. The active and reactive power balance is forced to zero by the bus voltage iterations.

Consider a system with $n+1$ buses. The first is a slack bus; buses 2 through $m-1$ are conventional load buses, and buses $m$ to $n$ have no sinusoidal loads. It is assumed that the active and reactive powers balance is known at each bus and that the nonlinearity is known. The power balance equations are constructed so that $\Delta P$ and $\Delta Q$ at all non slack buses is zero for all harmonics. The form of $\Delta P$ and $\Delta Q$, as a function of bus voltage and phase angle, is the same as in conventional load flow, except that $Y_{bus}$ is modified for harmonics. The current balance for fundamental frequency is written as:

$$\begin{bmatrix} I_{r,m} \\ I_{i,m} \\ - \\ I_{i,n} \end{bmatrix} = \begin{bmatrix} g_{r,m}(V_m^1, V_m^5, ........, \alpha_m, \beta_m) \\ g_{i,m}(V_m^1, V_m^5, ........, \alpha_m, \beta_m) \\ - \\ g_{i,n}(V_n^1, V_n^5, ........, \alpha_n, \beta_n) \end{bmatrix} \qquad (15)$$

Where $I_{r,m}$ and $I_{i,m}$ are real and imaginary bus injection currents at bus $m$ at the fundamental, $\alpha$ is the firing angle, and $\beta$ is the commutation parameter. This equation is modified for buses with harmonic injections as:

$$\begin{bmatrix} I_{r,1}^{k} \\ I_{i,1}^{k} \\ - \\ I_{i,m-1}^{k} \\ I_{r,m}^{k} \\ I_{i,m}^{k} \\ - \\ I_{i,n}^{k} \end{bmatrix} = - \begin{bmatrix} 0 \\ 0 \\ - \\ 0 \\ g_{r,m}^{k}\left(V_{m}^{1}, V_{m}^{5}, ..., \alpha_{m}, \beta_{m}\right) \\ g_{i,m}^{k}\left(V_{m}^{1}, V_{m}^{5}, ..., \alpha_{m}, \beta_{m}\right) \\ - \\ g_{i,n}\left(V_{n}^{1}, V_{n}^{5}, ..., \alpha_{n}, \beta_{n}\right) \end{bmatrix} \quad (16)$$

Where $I_{r,1}^{k}$ is the real and $I_{i,1}^{k}$ is the imaginary part of the current at the $k^{th}$ harmonic, $g_{i}^{k}$ and $g_{r}^{k}$ are the imaginary and real parts of the current equation at the $k^{th}$ harmonic and $V_{m}$ with superscript is the voltage at the harmonic.

The final equations for the harmonic power flow become:

$$\begin{bmatrix} \Delta W \\ \Delta I^{1} \\ \Delta I \\ \Delta I^{7} \\ ... \end{bmatrix} = \begin{bmatrix} J^{1} & J^{5} & J^{7} & .. & 0 \\ YG^{1,1} & YG^{1,5} & YG^{1,7} & .. & H^{1} \\ YG^{5,1} & YG^{5,5} & YG^{5,7} & .. & H^{5} \\ YG^{7,1} & YG^{7,5} & YG^{7,7} & .. & H^{7} \\ .. & .. & .. & .. & .. \end{bmatrix} \begin{bmatrix} \Delta V^{1} \\ \Delta V^{5} \\ .. \\ .. \\ \Delta \alpha \end{bmatrix}$$

$$(17)$$

Where all elements in equation (10) are sub-vectors and sub-matrices partitioned from $\Delta M$ (apparent mismatches), $J$, and $\Delta U$, i.e $\Delta M = J \Delta U$.

$\Delta W$ : mismatch active and reactive power.

$\Delta I^{1}$ : mismatch, fundamental current.

$\Delta I^{k}$ : mismatch, harmonic current at $k^{th}$ harmonic.

$J^{1}$ : conventional power flow Jacobian.

$J^{k}$ : Jacobian at harmonic $k$.

$$(YG)^{k,j} = Y^{k,k} + G^{k,k} (k = j)$$
$$= G^{k,j} (k \neq j) \quad (18)$$

Where $Y^{k,k}$ is an array of partial derivatives of injection currents at the $k^{th}$ harmonic with respect to the $k^{th}$ harmonic voltage, and $G^{k,j}$ are the partials of the $k^{th}$ harmonic load current with respect to the $i^{th}$ harmonic supply voltage; $H^{k}$ are the partial derivatives of no sinusoidal loads for real and imaginary currents with respect to $\alpha$ and $\beta$.

# 5 EXAMPLES

To illustrate the harmonic power flow algorithm, two examples are presented.

## 5.1 Example 1

It adopted the network in Fig.1. In which it has been selected one base of 100 KV and 100 MVA.

In this scheme, the generators respectively regulate the voltages of the buses 1 and 2 to the values of 1.06 (pu) and 1.04 (pu). The bus 1 is taken like oscillating bus whereas the node 2 is type PV with a generated power of 40 MW and one load PQ conventional of 20 and 10Mvar. The rest of the buses are of type PQ, having bus 4 one loads PQ conventional of 40 MW and 5 Mvar.
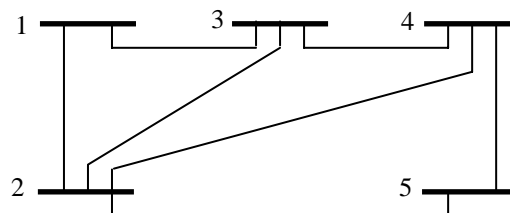


**Fig.1.** The network of five buses.

Table 1 Parameters of lines

| Lines | $R(pu)$ | $X(pu)$ | $B(pu)$ |
|-------|---------|---------|---------|
| 1-2 | 0.02 | 0.06 | 0.06 |
| 1-3 | 0.08 | 0.24 | 0.05 |
| 2-3 | 0.06 | 0.18 | 0.04 |
| 2-4 | 0.06 | 0.18 | 0.04 |
| 2-5 | 0.04 | 0.12 | 0.03 |
| 3-4 | 0.01 | 0.03 | 0.02 |
| 4-5 | 0.08 | 0.24 | 0.05 |

**Case 1:** System without non linear loads.

With these input data, is realised the fundamental load flow. For simulation a closing error of $10^{-5}$ has been used. Table 2 shows the results of voltages at fundamental load flow, before the incorporation of the load nonlinear.

Table 2 Fundamental load flow

| | $V_{k}(pu)$ | $\theta_{ik}(°)$ |
|-------|-------------|------------------|
| Bus 1 | 1.060 | 0.00 |
| Bus 2 | 1.040 | -2.40 |
| Bus 3 | 0.960 | -3.97 |
| Bus 4 | 0.960 | -4.14 |
| Bus 5 | 0.980 | -4.45 |

According to these results, there is a dynamic problem of stability and quality of voltages in buses 3, 4 and 5.

**Case 2:** System with non linear loads.

The loads nonlinear are connected respectively at buses 3, 4 and 5. Whereas the sub transitory reactance of the generators have a value of 0.125 pu
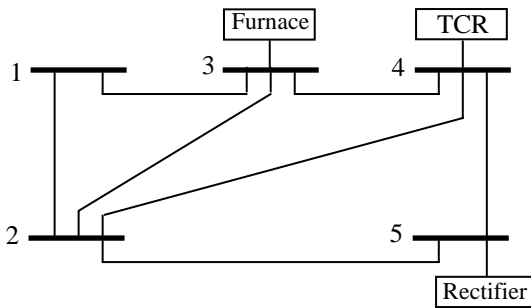


**Fig.2.** The network of five buses.

The nonlinear loads are defined of the following way:

The D-SVC with compensator TCR has a capacity of 100 MVAR to the nominal voltage of 100 KV; the point of operation is defined by means of a specific reactive power of 47.3 MVAR.

The installation of an electric furnace include a transformer 100 KV /700 V with the reactance x = 80% on the basis of the 100 MVA. The point of operation is adjusted while taking as consigns a current of 0.8 pu for the fundamental component.

The rectifier has a transformer of 100 KV/1KV, the reactance respectively take the values from the 20% to 80% on the basis of 100 MVA.

With these input data, is realised the load flow harmonic. For simulation, the 17 first harmonics characteristics were considered, i.e, until k=49, a closing error of $10^{-5}$ has been used. The determination of the passages by zero of control of firing in element TCR is made taking the fundamental component from voltage. The results of simulation are shown in Table 3 shows the harmonics currents generated by the loads nonlinear and from Table 4, can be observed the harmonics voltages in buses of the network.

Table3 Harmonics current absorbed by the no linear load

| Harmonic | | 1 | 5 | 7 | 11 | 13 | 17 | 19 |
|---|---|---|---|---|---|---|---|---|
| Bus 3 | $I_k(pu)$ | 80.00 | 2.79 | 1.82 | 1.12 | 0.80 | 0.10 | 0.68 |
| | $\theta_{ik}(°)$ | -50.93 | -169.20 | 103.51 | -58.88 | -142. | 48.26 | -17.58 |
| Bus 4 | $I_k(pu)$ | 49.26 | 3.40 | 1.72 | 0.88 | 0.82 | 0.17 | 0.57 |
| | $\theta_{ik}(°)$ | -94.42 | -122.12 | 56.39 | 22.03 | -143.57 | -164.83 | -2.59 |
| Bus 5 | $I_k(pu)$ | 51.02 | 11.10 | 4.72 | 2.96 | 2.11 | 0.56 | 1.32 |
| | $\theta_{ik}(°)$ | -39.61 | -19.73 | 90.26 | -71.01 | -150.58 | -133.51 | 166.09 |

Table4 Harmonics voltages at no linear loads

| Harmonic | | 1 | 5 | 7 | 11 | 13 | 17 | 19 |
|---|---|---|---|---|---|---|---|---|
| Bus3 | $V_k(pu)$ | 96.34 | 7.09 | 5.00 | 3.68 | 2.40 | 2.38 | 7.66 |
| | $\theta_{ik}(°)$ | -3.97 | -169.0 | 127.6 | 33.4 | -59.7 | -57.2 | 87.2 |
| Bus 4 | $V_k(pu)$ | 96.03 | 7.43 | 5.04 | 3.59 | 2.13 | 1.89 | 7.12 |
| | $\theta_{ik}(°)$ | -4.14 | -168.2 | 129.1 | 31.3 | -60.4 | -58.4 | 82.5 |
| Bus 5 | $V_k(pu)$ | 98.15 | 10.65 | 8.17 | 1.99 | 0.72 | 4.34 | 8.19 |
| | $\theta_{ik}(°)$ | -4.45 | -141.2 | 149.8 | 97.6 | 70.4 | 122.9 | -72.2 |

Table 5 Final values of the control variable

| | Harmonic load flow |
|---|---|
| Furnace | $V_{arc} = 296.57$ |
| Rectifier | $\alpha_0 = 28.56°$ |
| TCR | $\alpha_0 = 113.66°$ |

Table 6 Power at fundamental

|           | Harmonic load flow | |
|-----------|----------|----------|
|           | $P(MW)$ | $Q(M\,var)$ |
| Rectifier | 52.60    | 56.33    |
| TCR       | 40.94    | 28.83    |

The point of operation of the loads nonlinear comes defined by the final value that reaches the indicated control variables. In Table 5, is observed that the harmonics interaction appreciably modifies the firing angles of TCR.

On the other hand, discrepancies in the final values of the fundamental powers are obtained, for the furnace and the rectifier. This fact is shown in Table 6, where it is verified as it influences interaction harmonic in consummations PQ of the loads nonlinear.

Reliable results from technical point of view, an admissible distortion since it does not exceed the level of Electromagnetic compatibility established in the standards.

## 5.2  Example 2

This example is more complicated which adopted the network of 13 buses; the bus 1 is taken like oscillating bus whereas the node 6, 7, 8, 9 and 10 is type PV. The rest of the buses are of type PQ. The scheme and parameters of network is shown at Fig3 and in Tables 2 and 3.
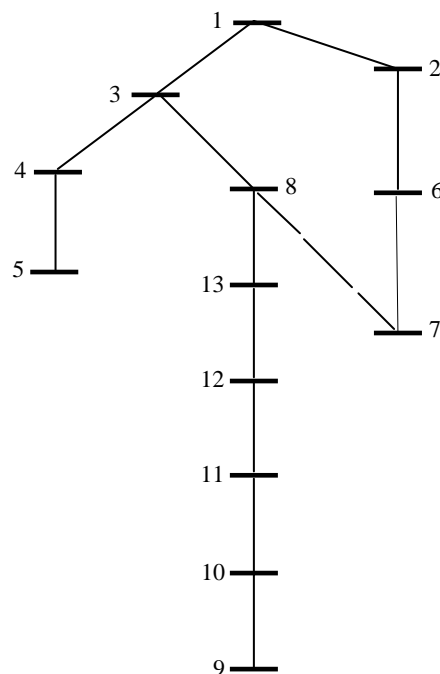


**Fig.3.** The network of 13 buses

Table 7 Parameters of lines

| Lignes | $R(pu)$ | $X(pu)$ | $B(pu)$ |
|--------|---------|---------|---------|
| 1-2    | 0.0042  | 0.08925 | 0.00    |
| 1-3    | 0.0044  | 0.10417 | 0.00    |
| 5-4    | 0.0044  | 0.10417 | 0.00    |
| 4-3    | 0.0074  | 0.14300 | 0.436   |
| 6-2    | 0.0481  | 0.4590  | 0.246   |
| 6-7    | 0.0090  | 0.1080  | 0.016   |
| 8-3    | 0.0121  | 0.2330  | 0.712   |
| 7-8    | 0.0000  | 0.1500  | 0.00    |
| 9-10   | 0.0105  | 0.2020  | 0.620   |
| 10-11  | 0.0000  | -0.1500 | 0.00    |
| 11-12  | 0.0086  | 0.16650 | 0.508   |
| 12-13  | 0.0075  | 0.14650 | 0.448   |
| 13-8   | 0.0000  | -0.1500 | 0.00    |

Table 8 Data Powers

| Bus | $P_{cons}(MW)$ | $Q_{cons}(M\,var)$ |
|-----|----------------|--------------------|
| 1   | 0.00           | 0.00               |
| 2   | 0.00           | 0.00               |
| 3   | 0.00           | 0.00               |
| 4   | 0.00           | 0.00               |
| 5   | 0.00           | 0.00               |
| 6   | -450.00        | 0.00               |
| 7   | 0.00           | 0.00               |
| 8   | 0.00           | 0.00               |
| 9   | -500.00        | 0.00               |
| 10  | 0.00           | 0.00               |
| 11  | 50.00          | 30.00              |
| 12  | 50.00          | 32.00              |
| 13  | 0.00           | 0.00               |

The per-unit (p.u) values of lines in the example system have been obtained for 66 KV and 10 MVA base values. The D-SVC with compensator TCR is connected to bus 9. There are no filters at all. The values in the application have been taken as per-unit; Hence the reactance of TCR $X_r = 0.25$ pu , capacitor reactance $X_c = 22.5$ pu

**Case 1:** The system without nonlinear loads.

In order to illustrate the accuracy of the program, the study was similar to the one discussed by Heydt et al [10].

With these input data, is realised the fundamental load flow. For simulation a closing error of $10^{-3}$ has been used. Table 9 shows the results of voltages at fundamental load flow, before the incorporation of the load nonlinear.

According to these results there is a dynamics problem of stability of voltages in bus 9.

Table 9 Fundamental load flow

|         | $V_k (pu)$ | $\theta_{ik} (°)$ |
|---------|-----------|-------------------|
| Bus 1   | 1.0000    | 0                 |
| Bus 2   | 1.0000    | -2.089            |
| Bus 3   | 1.0000    | -6.289            |
| Bus 4   | 1.0000    | -14.558           |
| Bus 5   | 1.0000    | -16.440           |
| Bus 6   | 1.0370    | -5.580            |
| Bus 7   | 1.0630    | -6.448            |
| Bus 8   | 1.1000    | -7.413            |
| Bus 9   | 0.9430    | -6.217            |
| Bus 10  | 1.1000    | -6.662            |
| Bus 11  | 1.0000    | -6.713            |
| Bus 12  | 1.0000    | -7.562            |
| Bus 13  | 1.0000    | -7.761            |

**Case 2:** The system with non linear loads.

The loads nonlinear are connected at buses 9.

Tables 10 and 11 illustrate the harmonics current absorbed by the no linear load, the harmonics voltages at no linear load, Table 12 is observed that the harmonics interaction appreciably modifies the firing angles of TCR. The results are very similar to the one obtained by the proposed methodology.
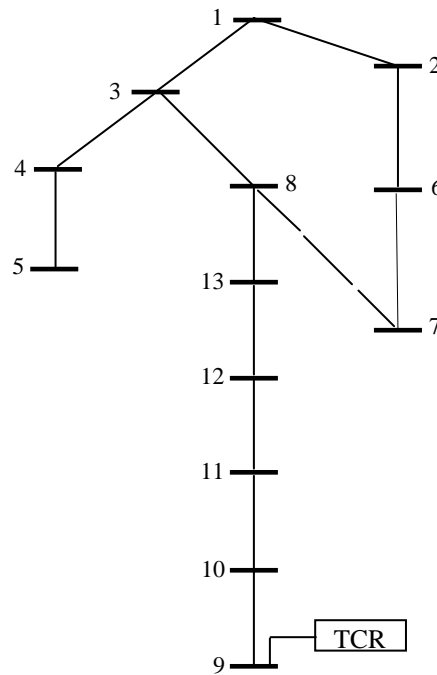


Fig.4.The network of 13 buses

Table 10 Harmonics current absorbed by the nonlinear load

| Harmonic |              | 1      | 5       | 7      | 11     | 13      | 17      | 19     |
|----------|--------------|--------|---------|--------|--------|---------|---------|--------|
| Bus 9    | $I_k (pu)$   | 50.1   | 2.98    | 1.58   | 0.90   | 0.71    | 0.15    | 0.55   |
|          | $\theta_{ik} (°)$ | -90.93 | -119.20 | 60.21  | 30.24  | -130.2  | -159.30 | -3.52  |

Table 11 Harmonics voltages at nonlinear loads

| Harmonic | | 1 | 5 | 7 | 11 | 13 | 17 | 19 |
|---|---|---|---|---|---|---|---|---|
| Bus 9 | $V_k\,(pu)$ | 94.30 | 6.95 | 4.55 | 3.68 | 2.35 | 2.20 | 7.66 |
| | $\theta_{ik}\,(°)$ | -3.12 | -165.2 | 119.1 | 25.3 | -56.2 | -46.2 | 73.1 |

Table 12 Final values of the control variable

| | Harmonic load flow |
|---|---|
| TCR | $\alpha_0 = 112.65°$ |

The study was actually carried to the 19 th harmonic, the program calculate the percent harmonic distortion (% HD) in the bus voltage (bus 9) and line current. We calculate also commutation angle at bus 9.

Note that in this example, significant harmonic distortion occurs in line current particularly at light loading.

The distortion factor is obtained gives the information nature of the voltage waveform at a system bus. Such information is of vital importance to a protection engineer in order to design an optimum protection system and avoid its malfunction due to the harmonics.

The distortion factor can be also be used to monitor the pollution of the frequency of the power system.

## 6  Conclusion

The analysis performed in this study indicates that the bus with nonlinear element is the one most affected by the harmonics. The reactive power compensation is very important in terms of voltage. Perfect compensation cannot be achieved when the effects of harmonics are not taken into consideration.

The simulation results show that there are significant harmonic distortions within the compensator system. When the system connected with distribution static VAR compensator including TCR is examined, it is noticed that some differences occur in critical values steady-state stability analysis depending on the presence of the harmonic component. This case clearly shows that harmonic components have non-negligible importance in stability and quality of voltage.

The program makes use of the virtual buses in the system and as a result the distribution voltage profile is made available. As shown in this paper such information can be used to investigate the standing wave pattern on distribution lines.

The distortion factor can also be used to monitor the pollution of the frequency of the power system.

In future, FACTS device (D-SVC) will be incorporated with another device in network of distribution.    .

*References:*
[1] J.G. Mayoredomo, Z. Zabala, A Contribution for Modelling Static VAR Compensators in Iterative Harmonic Analysis, *International Conference on Harmonics and Quality of Power ICHQP 98, jointly organized by IEEE/PES and NTUA*, Athens, October 14-16, 1998.

[2] M. Uzunoglu, Harmonic and voltage stability analysis in power systems including thyristor-controlled reactor, *Sadhana*, Vol. 30, Febrruary 2005, pp.57-67.

[3] D. Xia, and G.T. Heydt, Harmonic power flow studies, Part I – Formulation and solution, *IEEE Trans. Power Apparatus and systems*, Vol. PAS-101, No. 6, June 1982, pp.1257-1265.

[4] D. Xia, and G.T.Heydt, Harmonic power flow studies, Part II – Implementation and Practical Application, *IEEE Trans. Power Apparatus and systems*, Vol. PAS-101, No. 6, June 1982, pp.1266-1270.

[5] Xu. Wenyuan Jose, R. Marti, and W. Domme, A Multiphase Harmonic Load Flow Solution Technique, *IEEE Transactions on Power Systems*, Vo1.6, No.1, February 1991.

[6] A. Enrique, R.Clodio, H. Fuerte-Esquivel, Ambriz-Perez, C Angeles-Camacho, Modelling and Simulation in Power Networks, *JOHN WILY & SONS*, LTD, 2004.

[7] G.T. Heydt, ,W.M. Grady , D. Xia, Harmonic Power Flow Studies, Vol 1, Theoretical Basis, EPRI EL 3300, Project 1764-7 Electric Power Research Institute, Palo Alto, CA, November 1983.

[8] G.T Heydt, W.M Grady, D. Xia, Distributed loads in Electric Power Systems, *IEEE Trans.* Vol. PAS-103, No. 6, June 1985, pp.1385-1390.

[9] H. Amhriz-PBrez, E. Acha, and C. R. Fuerte-Esquivel, Advanced SVC Models for Newton-Raphson Load Flow and Newton Optimal Power Flow Studies, Vol. 15. No. 1, February 2000.

[10] G.T. Heydf, W.M. Grady, D. Xia, Harmonic Power Flow Studies Volume 1: Theoretical Basis, Electric Power Research Institute, *EPRI EL3300*, Project 1764-7. Final Report, November, 1983.

[11] W.Xu, J.R.Marti and H.W.Dommel, Harmonic analysis of systems with Static Compensators, *Paper submitted for IEEE PES*. Winter Meeting 1990.

[12] W.Xu, J.R.Marti and H.W.Dommel, Compensation of Steady State harmonics of Static Var Compensators, *Proc. of the Third International Conference on Harmonics in Power Systems*, Nashville,IN?pp.239-245, Oct. 1998.

[13] N. Li, Y. Xu, H. Cheng, FACTS-Based Power Flow Control in Interconnected Power Systems, IEEE Transactions on Power Systems, 2000.

[14] T. Orfanogianni, A flexible software environment for steady-state power flow optimization with series FACTS devices, *Diss. ETH Nr. 13689, EEH – Power System laboratory* ETH Zurich 2000.

[15] W. E. Reid and K. J. Petrus, Harmonics and capacitors in the power system, in *Proc. Pacsfic Coast Elect. Assoc. Eng. Operating Conf.* (Los Angeles, CA), Mar. 1985.

[16] W.S. Vilcheck and D.A.Gonzalez , Measurement And simulations combined for state of art harmonic analysis, in prod. Oct 1988, pp.1530-1534.

[17] J Arrillaga, C P Arnold, Harker B J 1983 Computer modelling of electrical power system, (Norwich: John Wiley & Sons.

[18] H Jagabondhu and K. S Avinash , A new power flow model incorporating effects of automatic controllers, WSEAS TRANSACTIONS on POWER SYSTEMS, Issue 8,Volume 2, August 2007.

[19] H.Yang, Mansoor, Y. Gang, Z. LI-Dan, C. Chen, Harmonic Mitigation of Residential Distribution System using a Novel Hybrid Active Power Filter, WSEAS TRANSACTIONS on POWER SYSTEMS, , Issue 12,Volume 2, december 2007.

[20] H. Walid, Y. G. Hegazy M. A. Mostafa, and M. A. Badr, Strategy Placement of Distributed Generation Units to Avoid Load Shedding in Overloaded Power Systems, WSEAS TRANSACTIONS on POWER SYSTEMS, , Issue 12,Volume 2, December 2007.